

## DSMC SIMULATION OF TRANSITION AND TURBULENT FLOW IN A LID-DRIVEN CAVITY AT HIGH MACH NUMBER

S. Pradhan and V. Kumaran

Department of Chemical Engineering, Indian Institute of Science, Bangalore- 560 012, India

### Abstract

*The flow in a 2D and 3D lid-driven cavity, with two opposite walls moving in opposite directions with equal velocity, simulated using the direct simulation Monte Carlo (DSMC) method, has been used as a test bed for examining different aspects of transition and turbulence [1, 2, 3, 4, 5, 6, 7, 8, 9, 10, 11, 12, 13, 14] at high Mach  $M = (U_w / \sqrt{k_B T_w / m})$  and Reynolds numbers  $Re = (\rho_{av} U_w L_y / \mu_w)$ . Here,  $L_y$  is the smallest box dimension,  $U_w$  and  $T_w$  are the wall velocity and temperature,  $\rho_{av}$  is the volume-averaged gas density, and  $\mu_w$  is the gas viscosity at the temperature corresponding to the wall temperature.*

*The transition is found to be highly sub-critical in 2D even at high Mach number, with well-separated lower and upper critical Reynolds numbers for the transition from turbulent-laminar and laminar-turbulent transitions. The transition Reynolds number increases faster than linearly with Mach number. This implies that the Knudsen number at transition (ratio of mean-free-path and system size, also proportional to the ratio of Mach and Reynolds numbers) passes through a maximum as the Mach number is increased. This maximum value is small, less than 0.025, indicating that transition is a continuum phenomenon even at high Mach numbers. The transition to turbulence is sub-critical in 3D as well. The transition Reynolds number does increase with Mach number, and the Knudsen number increases monotonically with Mach number over the parameter range studied here.*

*In the present analysis of high Mach turbulent flows using DSMC method, wall slip in the temperature and the velocities are found to be significant. Slip occurs because the temperature/velocity of the molecules incident on the wall could be very different from that of the wall, even though the temperature/velocity of the reflected molecules is equal to that of the wall (Pradhan & Kumaran, J. Fluid Mech-2011). There is slip even in the mean velocity as well as the intensity of the turbulent velocity fluctuations tangential to the wall. Due to the non-zero variation in the tangential velocities, it is found that the wall-normal fluctuating velocity increases proportional to the distance from the wall, in contrast to an incompressible flow with no-slip boundary conditions where the velocity increases as the square of the distance from the wall. We find that the amplitudes of the tangential fluctuating velocities increase close to the one-third power of the distance from the wall.*

*In a compressible turbulent flow, we examine the result that the ratio of the mean free path ( $\lambda$ ) and Kolmogorov scale ( $\eta$ ) increases proportional as  $(M/Re^{1/4})$ , and it increases asymptotically with Mach number in the high Mach number limit. The simulation show that the ratio does decrease as  $Re^{-1/4}$ , but it does not increase linearly with Mach number. The resolution suggested by our simulation is that even though the Mach number based on the wall velocity and temperature is large, the local Mach number based on the local dissipation velocity in regions of high shear decreases due to an increase in temperature. Due to this, the ratio of the mean free path and Kolmogorov scale appears to taper off in the high Mach number limit.*

*An important finding is that the ratio of the mean free path and Kolmogorov scale shows very little variation across the domain, even though the mean free path and Kolmogorov scale individually show larger variations. The ratio of the mean free path and Kolmogorov scale was also shown to be*

*equal to the local Mach number based on the local dissipation velocity, and can also be interpreted as the square root of the ratio of the strain rate and collision frequency. All of these quantities are remarkably invariant across the domain, indicating a coupling between the local temperature and the dissipation rate in a high Mach number turbulent flow.*

**Key Words:** Transition and turbulence, Compressible flows, Lid-driven cavity, DSMC simulations.

## 1. Introduction

A molecular simulation technique, the direct simulation Monte-Carlo (DSMC) algorithm (Bird (1994)), is used to study different aspects of transition and turbulence in the flow in a ‘lid-driven cavity’. Here, the flow in a two-dimensional rectangular, or three-dimensional cubic, cavity is driven by the opposing motion of two opposite walls. A specific aspect ratio,  $L_x : L_y : L_z = 1.96 : 1 : 1$  is chosen to facilitate comparison with previous studies, but we expect the qualitative features reported here to be more general. Our study is restricted to a maximum Reynolds number of about  $10^4$  and a maximum Mach number of 20. Though molecular simulations are more computationally intensive than continuum simulations, however, there are several advantages to using molecular simulations. It is possible to probe aspects related to the ratio of the mean free path and the characteristic flow scales (Kolmogorov scale, viscous sub-layer thickness) which are not accessible in the continuum approximation. Non-continuum effects such as wall velocity slip (fluid velocity at the wall different from wall velocity) and temperature slip (gas temperature at the wall different from wall temperature), which need to be modeled in a continuum formulation, result naturally from the molecule-wall collision law in the DSMC simulations. A problem specific to Navier-Stokes solutions of lid-driven cavity flows, the logarithmic divergence of the force on the wall with the grid resolution due to the velocity discontinuity at the corners, is not present in the DSMC simulation.

The DSMC method uses a probabilistic Monte-Carlo algorithm for simulating the Boltzmann equation for the velocity distribution function in dilute gases. Due to the use of the molecular chaos approximation in the Boltzmann equation, the simulation is restricted to the ideal gas limit. In the DSMC algorithm, the evolution of the positions and velocities of ‘simulated molecules’, each of which represents a large number of real molecules, is followed in time and space. Inter-molecular interactions are modeled using a probabilistic model which reproduces correctly the variation of macroscopic properties, such as the pressure and viscosity.

In the present study, we define the transition from a ‘laminar’ to a ‘turbulent’ flow based on the discontinuity in the net force (or average shear stress) on the moving walls in the three-dimensional flow. Though this is not a microscopic definition, it is unambiguous. Continuous bifurcations to more complex flows which occur upon an increase in Reynolds number will alter the slope of the force-Reynolds number curve, but will not result in a discontinuity. In our simulations, we do observe a discontinuity coupled with hysteretic behavior in 2D, indicating a sub-critical transition. Along with the force discontinuity, there is also a discontinuity in the mean velocity profile, and in the mean square of the fluid velocity fluctuations. Moreover, there is hysteresis even in a 3D lid-driven cavity; the discontinuity for increasing Reynolds number occurs at a higher Reynolds number than that for decreasing Reynolds number. The sub-critical nature of the transition and the hysteresis are qualitatively similar to that in channel and pipe flows, and they indicate that the transition is not likely to be captured by simple linear stability studies.

The fluid is a hard sphere gas with the molecular diameter  $d = 4.17 \times 10^{-10}$  m, and molecular mass  $m = 6.63 \times 10^{-26}$  kg/molecule and specific heat ratio  $\gamma = 1.66$  corresponding to argon atoms. The hard sphere (HS) molecular model is used in the simulations. It is assumed that the gas molecules undergo diffuse reflection from all the solid surfaces with the thermal accommodation coefficient equal to 1. The wall temperature is maintained at 300 K.

## 2. Validation

First, we validate the 2D-DSMC results at subsonic flow conditions ( $Ma= 0.2$ ) with the experimental results of Kuhlmann, Wanschura & Rath (1997), in Figure 1. The variation of normalized y-component of velocity, ( $v/v_{max}$ ), along x-coordinate is shown in Figure 1. The DSMC simulation results are compared with the experimental results of Kuhlmann, Wanschura & Rath (1997) for two different types of flows, the two vortex flow and the cat's eye flow. It is found that there is quantitative agreement between the simulation and experimental results.

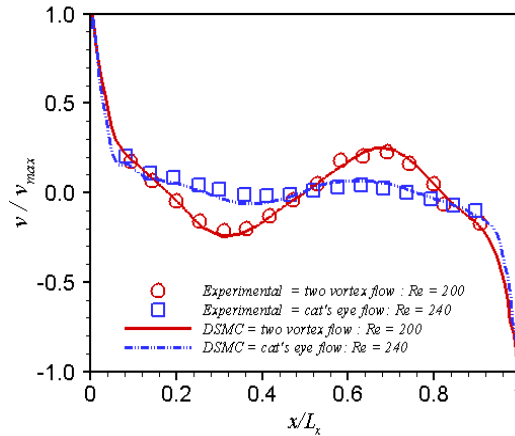


Figure 1. Comparison between 2D DSMC simulations, and experiments of Kuhlmann, Wanschura & Rath (1997) for the normalised y-component velocity ( $v/v_{max}$ ) along x-coordinate at ( $y/L_y = 0.5$ ), for the two vortex flow at  $Re = 200$  and cat's eye flow at  $Re = 240$ .

An important issue in the driven-cavity flow is the singularity in the wall stress at the corner between the moving and the fixed walls, due to the velocity discontinuity. The wall stress diverges as the inverse of the distance from the corner, and consequently the force on the wall is infinite. In discrete (finite difference/element) simulations, the force on the wall increases proportional to the logarithm of the inverse of the grid spacing, or proportional to the logarithm of the number of grid points. The stress singularity can be resolved only by recognizing that the continuum approximation is not valid when the distance from the corner is smaller than the mean free path, and it is necessary to resolve the molecular motions very close to the corners. Since the DSMC simulations do resolve the mean free path, there is no stress singularity or force divergence. In the DSMC simulations, the divergence is cutoff due to the discrete nature of the simulations. Figure 2 shows the average force as a function of the number of cells for the 3D simulations. In addition, there is very little dependence on the average force per unit area on the number of simulated molecules per cell, provided the latter is sufficiently large.

In the DSMC simulations, if the number of simulated molecules per cell,  $n$ , is small, the average properties do depend on  $n$ . However, it is expected as  $n$  increases, the average properties will converge to a constant value independent of  $n$ , which is the value of the property in the continuum approximation. This dependence is studied for the mean and root mean square of the fluctuating velocities for the turbulent flow in a three-dimensional lid-driven cavity as a function of the inverse of the number of simulated molecules per cell at Reynolds number  $10^4$  and Mach number 5 in Figure 3.

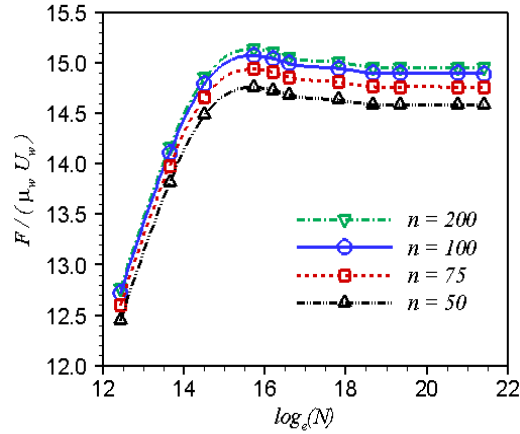


Figure 2. Force per unit area on the moving wall normalized by  $(\mu_w U_w)$ , as a function of logarithm of number of cells ( $N$ ) at  $M = 5$ ,  $Re = 10^4$  for different number of simulated molecules per cell ( $n$ ).

It should be noted that in the simulation, the total number of real molecules is kept constant, and the ratio of the numbers of real and simulated molecules is varied. The magnitude of the mean and root mean square velocities do decrease as the number of simulated molecules is increased, but they reach a constant limiting value in the limit  $n \rightarrow \infty$ . As number of simulated molecules per cell ( $n$ ) increases, the mean-square velocity fluctuation decreases, and appears to be proportional to  $(1/n)$  for small  $n$ .

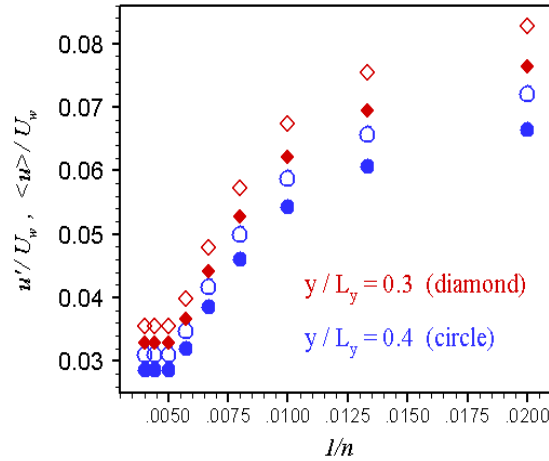


Figure 3. Mean and root mean square velocity fluctuations as a function of  $(1/n)$  at different  $y$  locations for  $Re = 10^4$  and  $M = 5$ , for  $(u', \langle u \rangle)$ . The symbols show the DSMC results at  $(x/L_x = 0.5, z/L_z = 0.5)$ , and for  $(y/L_y) = 0.3$  (diamond) and  $(y/L_y) = 0.4$  (circle). The filled symbols are for the mean velocities, and the open symbols are for the root mean square of the fluctuating velocities.

### 3. Two and Three dimensional flow

We analyze the effect of Mach number on the flow transition in two dimensions for Mach numbers up to 20. The transition is indicated by a discontinuous change in the strain rate along the moving wall. The transition is clearly subcritical, with an upper bifurcation point (UBP) for the transition from two-vortex to cats-eye flow as the Reynolds number is increased, and a lower bifurcation point (LBP) for the reverse transition when the Reynolds number is decreased. The streamlines for the two-vortex and cats-eye flow are qualitatively similar to those for the incompressible flow. However, there is a monotonic increase in the transition Reynolds number for both the lower and upper bifurcation points. Over the range of Mach numbers studied, we find that the transition Reynolds number for both the upper and lower bifurcation points are very well expressed as a

quadratic function of the Mach number. The streamlines for the two-vortex flow, cats-eye flow, and elliptic vortex at Mach number 5 is shown in Figure 4.

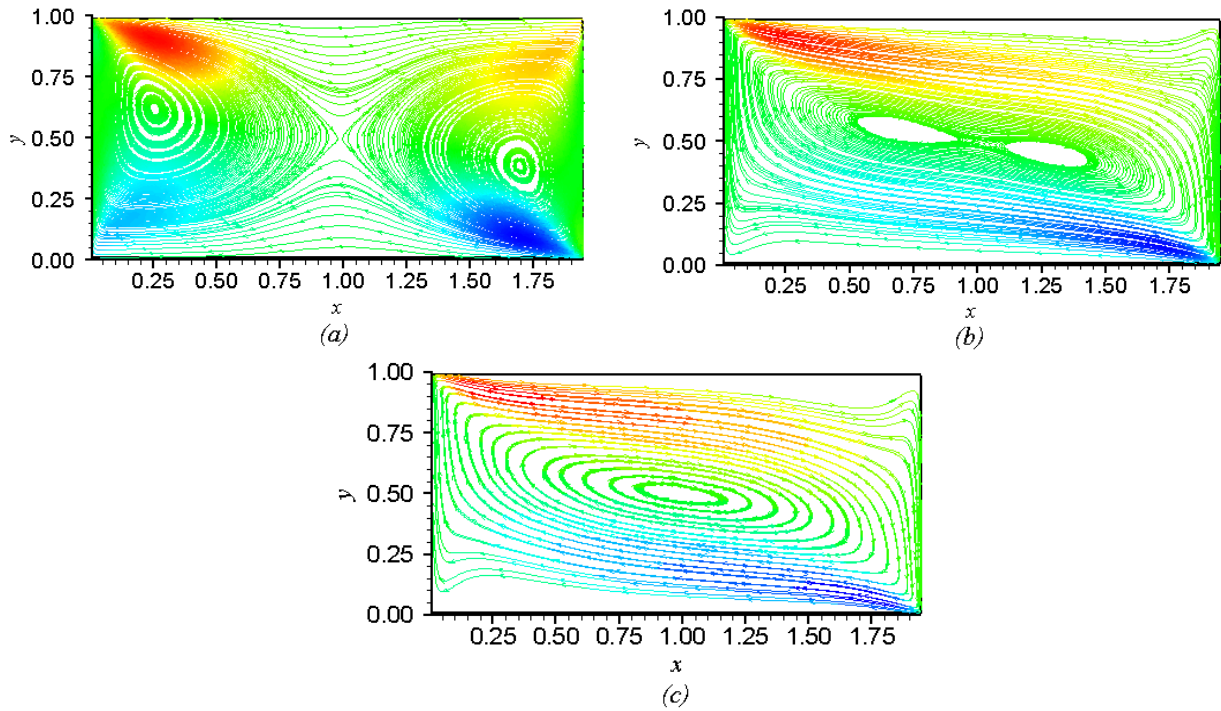


Figure 4. Flow bifurcation in a 2D lid-driven cavity; two vortex flow at  $Re = 200$  (a), cat's eye flow at  $Re = 350$  (b), and elliptic vortex at  $Re = 1850$  (c), at  $M = 5$ .

The transition Knudsen number as a function of Mach number for the upper bifurcation point and lower bifurcation point in 2D DSMC simulations is shown in Figure 5(a), and for the laminar-turbulent transition and turbulent-laminar transition in 3D-DSMC simulations is shown in Figure 5(b).

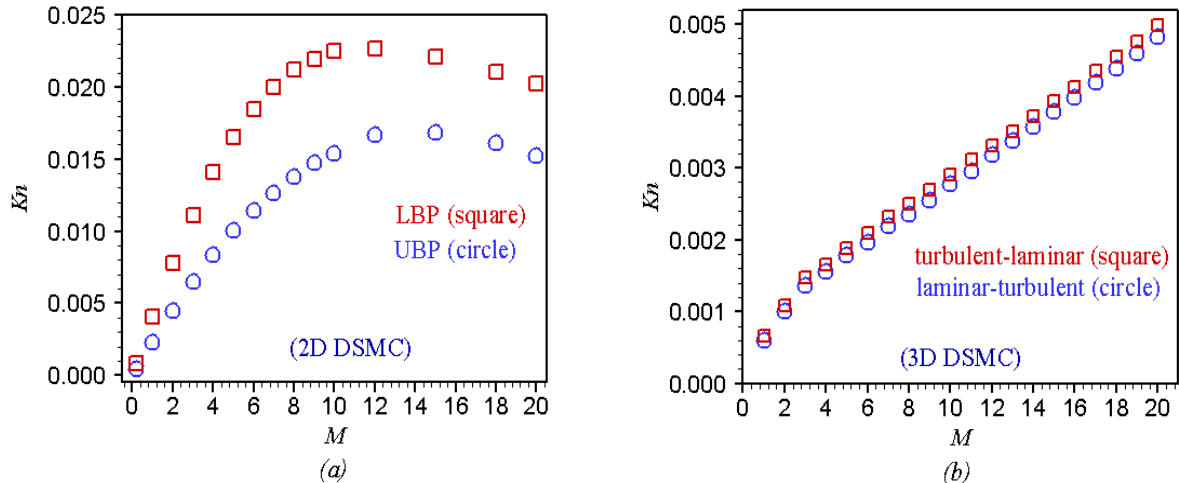


Figure 5. Variation of transition Knudsen number as a function of Mach number for the upper bifurcation point (circle) and lower bifurcation point (square) in 2D DSMC (a); and for the laminar-turbulent transition (circle) and turbulent-laminar transition (square) in 3D-DSMC (b).

The variation of Kolmogorov scale  $\eta = (v^3/\epsilon)^{1/4}$  and the ratio of mean free path to Kolmogorov scale ( $\lambda/\eta$ ), is plotted at different spatial locations in figure 6 (a), (b). Figure 6 (a) shows that there is

a large variation in the Kolmogorov scale, by a factor of 2 – 3, across the domain. However, figure 6(b) shows that the variation ( $\lambda/\eta$ ) is relatively small; the variation is less than 5% in the region  $0.2 < (x/L_x) < 0.8$ , though there is a somewhat larger variation near the walls. This suggests a coupling between the Kolmogorov scale and the mean free path in a compressible turbulent flow. The ratio of the mean free path and the Kolmogorov scale, ( $\lambda/\eta$ ), is the Knudsen number based on the Kolmogorov scale. This ratio is also proportional to the Mach number based on the local dissipation velocity.

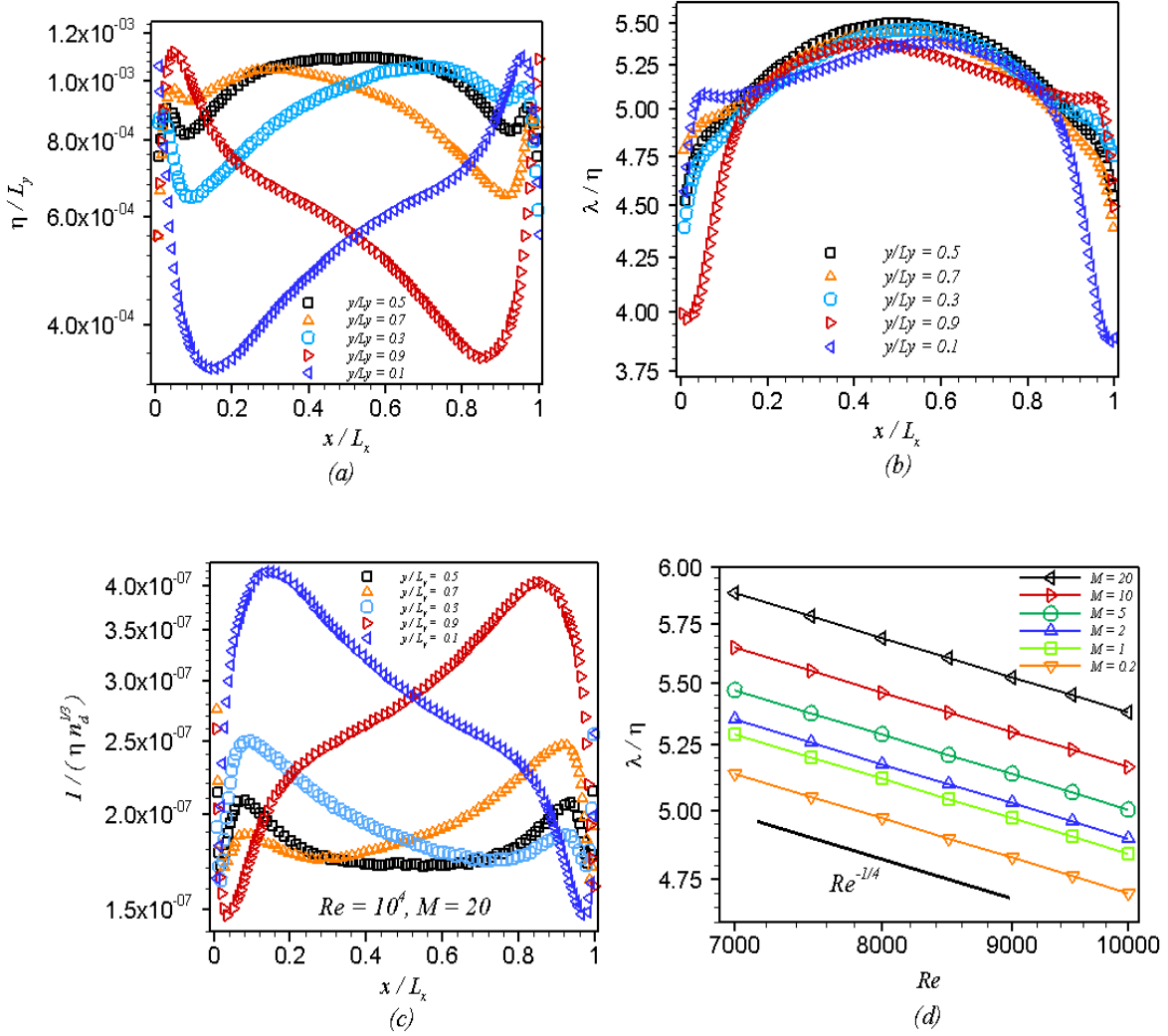
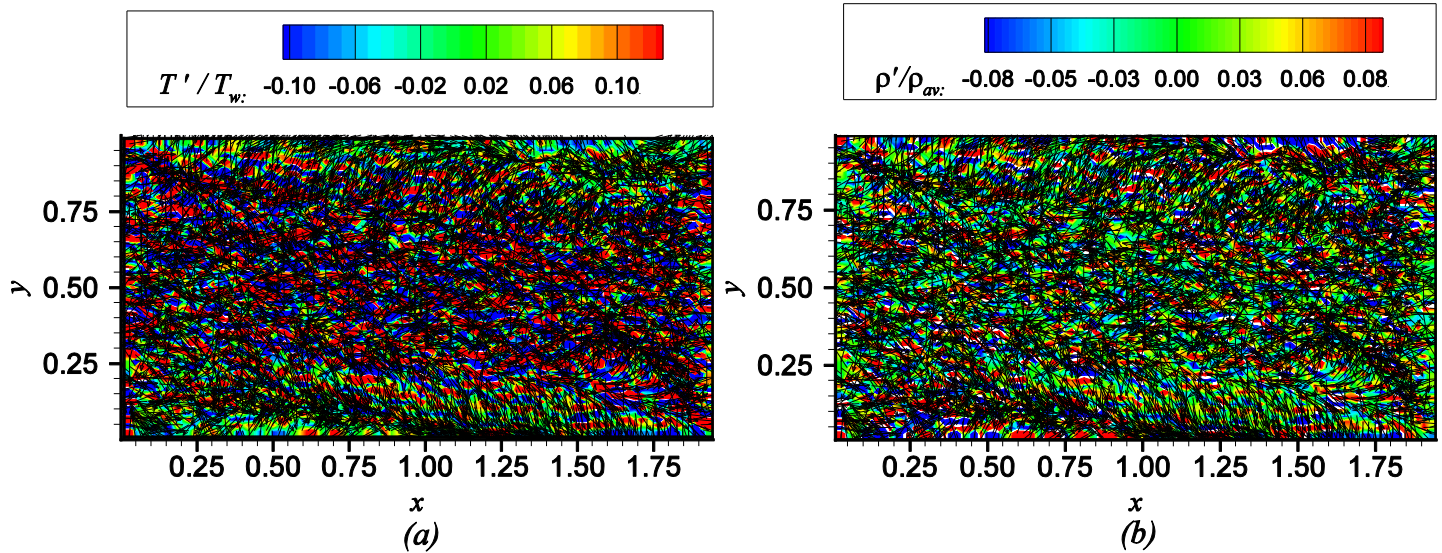


Figure 6. The scaled Kolmogorov length scale (a), the ratio of mean free path to Kolmogorov scale (b), the ratio of the mean molecular spacing to Kolmogorov scale (c) along  $x$ , at  $(z/L_z) = 0.5$ , and at different  $y$  locations for  $Re = 10^4$ , and  $M = 20$ ; and the ratio of mean free path to Kolmogorov scale as a function of  $Re$ , averaged over the region  $0.2 \leq (x/L_x) \leq 0.8$  and  $0.2 \leq (y/L_y) \leq 0.8$  at the location  $(z/L_z) = 0.5$  (d) in a 3D lid-driven cavity.)

A counter-intuitive result obtained is that the Kolmogorov scale could be smaller than the mean free path. The comparison should be made carefully, because the Kolmogorov scale is not exactly defined, and there is a range of scales over which dissipation takes place. The mean free path is known more exactly, since we can measure the actual distance between collisions. Despite this, it

still seems unusual that the mean free path is becoming larger than the smallest flow scales. This can be partially explained by realizing that cell size in the simulations is smaller than the mean free path, but it still contains a sufficiently large number of molecules so that the continuum approximation can be used. It is possible to find an intermediate scale because the distance between molecules is much smaller than the mean free path. The distance between molecules is proportional to  $n_d^{-1/3}$ , where  $n_d$  is the number density of the molecules. The mean free path, which is the distance between collisions, is much larger than the distance between molecules, due to the small probability that two nearest molecules are moving towards each other. The ratio of the distance between molecules and the mean free path is proportional to  $(n_d^{-1/3} n_d d^2) \sim (n_d d^3)^{2/3}$ , which is proportional to  $\phi^{2/3}$ , where  $\phi$  is the volume fraction of the molecules. Since the volume fraction is small for a dilute gas, the distance between molecules could be much smaller than the mean free path. We have verified, in the simulations, that the Kolmogorov scale is much larger than the distance between molecules. In figure 6(c), the ratio mean molecular spacing to Kolmogorov scale ( $1/(\eta n_d^{1/3})$ ) is plotted along  $x$  at different locations of  $y$  for  $Re = 10^4$ ,  $M = 20$  with 8 sub-cells per cell. This ratio is much less than 1, indicating that the continuum approximation could be used even when over length scales smaller than the mean free path. Thus, it is possible to have a continuum Kolmogorov scale smaller than the mean free path. Figure 6 (d) shows that  $(\lambda/\eta)$ , averaged across the interior of the cavity excluding 20% of the volume adjacent to the walls, is indeed proportional to  $Re^{-1/4}$  for the entire range of Mach numbers studied here.

The temperature, density, and velocity fluctuations with fluctuating velocity vectors are shown in Figure 7 for  $Re = 10^4$ , and  $M = 20$  (turbulent state) on  $(x-y)$ -plane at  $z/L_z = 0.5$ .



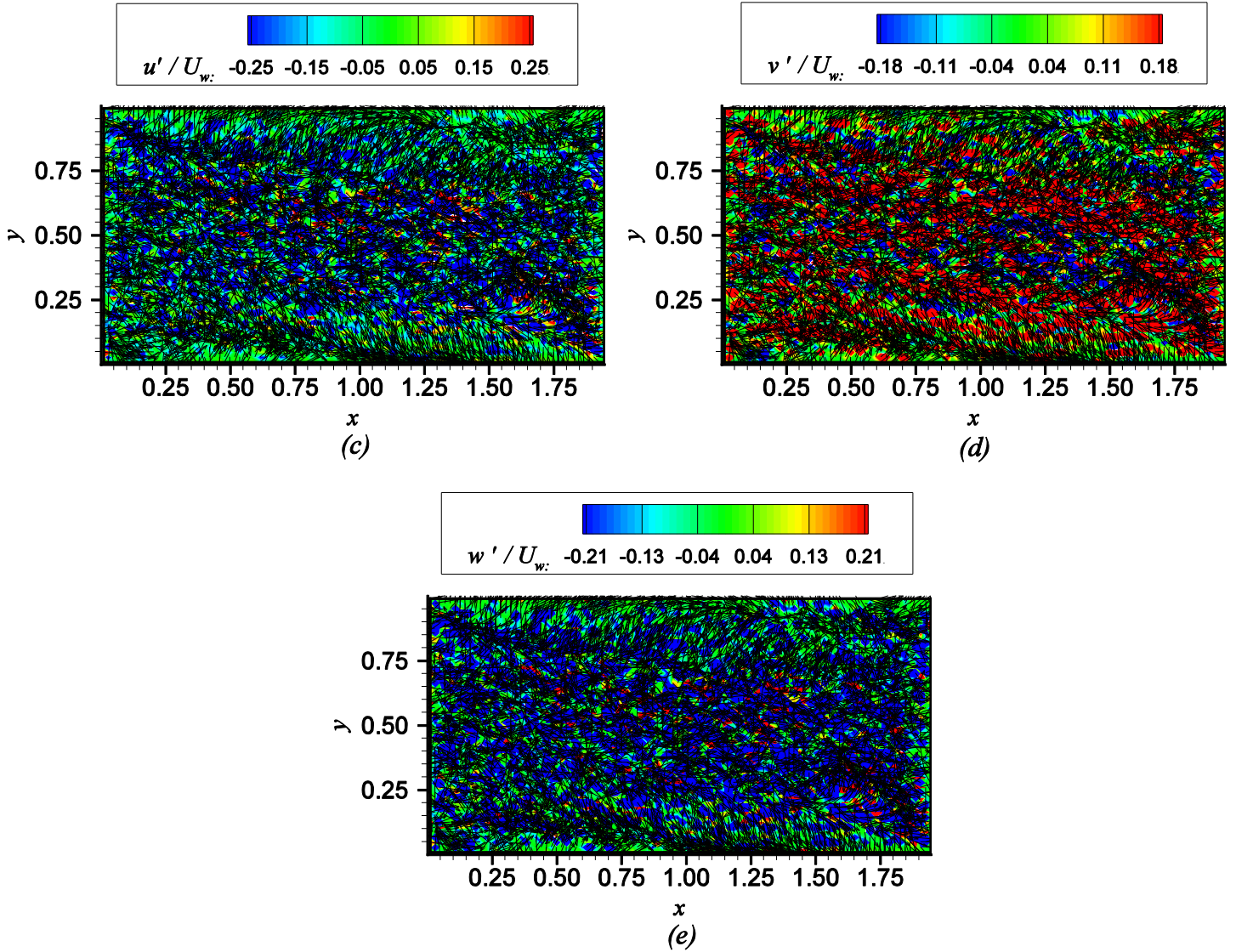


Figure 7. The temperature fluctuations (a); density fluctuations (b); and the velocity fluctuations ( $u'/U_w$ ) (c); ( $v'/U_w$ ) (d); ( $w'/U_w$ ) (e) with fluctuating velocity vectors for  $Re = 10^4$ , and  $M = 20$  (turbulent state) on ( $x$ - $y$ )-plane at  $z/L_z = 0.5$ .

#### 4. Conclusions

The direct simulation Monte Carlo method is used to simulate the transition and turbulence characteristics in a compressible lid-driven flow. The transition is found to be highly sub-critical in 2D even at high Mach number, with well-separated lower and upper critical Reynolds numbers for the transition from turbulent-laminar and laminar-turbulent transitions.

In a compressible turbulent flow, we examine the result that the ratio of the mean free path and Kolmogorov scale increases proportional as  $(M/Re^{1/4})$ , and it increases asymptotically with Mach number in the high Mach number limit. The simulation show that the ratio does decrease as  $Re^{-1/4}$ , but it does not increase linearly with Mach number. The resolution suggested by our simulation is that even though the Mach number based on the wall velocity and temperature is large, the local Mach number based on the local dissipation velocity in regions of high shear decreases due to an increase in temperature. Due to this, the ratio of the mean free path and Kolmogorov scale appears to taper off in the high Mach number limit.



Even though the distance between molecules is the smallest length scale for gradients, the mean free path is the length scale for molecular transport, since the kinematic viscosity and thermal conductivity are proportional to the product of the mean free path and the fluctuating velocity. The present results suggest that the smallest scale for transport could be much larger than the smallest scale for gradients, thereby suggesting non-local transport in high Mach number turbulent flows at the smallest scales.

## References

- [1] Bird, G. A. 1994. *Molecular gas dynamics and the direct simulation of gas flows*. Clarendon Press, Oxford.
  - [2] Bird, G. A. 1963 Approach to translational equilibrium in a rigid sphere gas. *Phys. Fluids* 6, 1518.
  - [3] Bradshaw, P. 1977 Compressible turbulent shear layers. *Annu. Rev. Fluid Mech.* 9, 33.
  - [4] Chapman, S. & Cowling, T. G. 1952 *The Mathematical Theory of Non-Uniform Gases*, 2<sup>nd</sup> edition. Cambridge, Cambridge University Press.
  - [5] Davidson, P. A. 2007 *Turbulence*. Oxford university Press.
  - [6] Huang, P. G. & Coleman, G. N. 1994 Van Driest transformation and compressible wall-bounded flows. *AIAA J.* 32(10), 2110.
  - [7] Kuhlmann, H. C., Wanschura, M., & Rath, H. J. 1997. Flow in two-sided lid-driven cavities: non-uniqueness, instabilities, and cellular structures. *J. Fluid Mech.* 336, 267.
  - [8] Morkovin, M. V. 1962 Effects of compressibility on turbulent flows. In *Mecanique de la Turbulence* (ed. A. Favre) CNRS., 367.
  - [9] Moffatt, H. K. 1964 Viscous and resistive eddies near a sharp corner. *J. Fluid Mech.* 18, 1.
  - [10] Pradhan, S. & Kumaran, V. 2011 The generalized Onsager model for the secondary flow in a high-speed rotating cylinder. *J. Fluid Mech.* 686, 109.
  - [11] Prasad, A. K. & Koseff, J. R. 1989 Reynolds number and end-wall effects on a lid-driven cavity flow. *Phys. Fluids A.* 1, 208.
  - [12] Shankar, P. N. & Deshpande, M. D. 2000 Fluid mechanics in the driven cavity. *Annu. Rev. Fluid Mech.* 32, 93.
  - [13] Tennekes, H. & Lumley, J. L. 1972 *A First course in turbulence*. Cambridge, The MIT Press.
  - [14] Van Driest. 1951 Turbulent boundary layer in compressible fluids. *J. Aero. Sci.* 18(3), 145.
-